

Seasonal variations of leaf area index of agricultural fields retrieved from Landsat data

M.C. González-Sanpedro ^{a,b,*}, T. Le Toan ^{a,1}, J. Moreno ^{b,2}, L. Kergoat ^{a,1}, E. Rubio ^{c,3}

^a Centre d'Etudes Spatiales de la Biosphère, CESBIO (CNES, CNRS, IRD, UPS), 18 avenue Edouard Belin, F-31401 Toulouse Cedex 9, France

^b Department of Earth Physics and Thermodynamics, University of Valencia, Valencia, Spain., Dr. Moliner, 50, 46100, Burjassot (Valencia), Spain

^c Instituto de Desarrollo Regional (IDR), University of Castilla-La Mancha, Campus Universitario, s/n, 02071 Albacete, Spain

Received 20 July 2006; received in revised form 18 June 2007; accepted 22 June 2007

Abstract

The derivation of leaf area index (LAI) from satellite optical data has been the subject of a large amount of work. In contrast, few papers have addressed the effective model inversion of high resolution satellite images for a complete series of data for the various crop species in a given region. The present study is focused on the assessment of a LAI model inversion approach applied to multitemporal optical data, over an agricultural region having various crop types with different crop calendars. Both the inversion approach and data sources are chosen because of their wide use. Crops in the study region (Barrax, Castilla–La Mancha, Spain) include: cereal, corn, alfalfa, sugar beet, onion, garlic, papaver. Some of the crop types (onion, garlic, papaver) have not been addressed in previous studies. We use in-situ measurement sets and literature values as a priori data in the PROSPECT+SAIL models to produce Look Up Tables (LUTs). Those LUTs are subsequently used to invert Landsat-TM and Landsat-ETM+ image series (12 dates from March to September 2003). The Look Up Tables are adapted to different crop types, identified on the images by ground survey and by Landsat classification. The retrieved LAI values are compared to in-situ measurements available from the campaign conducted in mid July-2003. Very good agreement (a high linear correlation) is obtained for LAI values from 0.1 to 6.0. LAI maps are then produced for each of the 12 dates. The LAI temporal variation shows consistency with the crop phenological stages. The inversion method is favourably compared to a method relying on the empirical relationship between LAI and NDVI from Landsat data. This offers perspectives for future optical satellite data that will ensure high resolution and high temporal frequency.

© 2007 Elsevier Inc. All rights reserved.

Keywords: Landsat multitemporal; LAI; SAIL; Biophysical parameters retrieval

1. Introduction

Monitoring agricultural crops during the growing season becomes increasingly important in order to adjust the management (e.g. irrigation, fertilizers) and to provide infor-

mation for obtaining yield predictions before harvest time. Crop growth models and soil–vegetation–atmosphere process models are more and more used for such monitoring activities. However, it is difficult for the models to account for the spatial heterogeneity in vegetation and soil conditions as well as the inherent difficulties of phenology modelling. One solution consists in calibrating the models using measurements of biophysical parameters (e.g. Brisson et al., 1998; Bondeau et al., 1999; Launay & Guerif, 2005; Spitters et al., 1989).

For calibrating crop growth models, a key variable is the leaf area index (LAI), which accounts for the leaf surface intercepting in-coming radiation. LAI stands out because it takes part in functioning processes through the allocation of carbon to leaves. LAI is also involved in the description of soil–vegetation–atmosphere exchanges like evapotranspiration,

* Corresponding author. Centre d'Etudes Spatiales de la Biosphère, CESBIO (CNES, CNRS, IRD, UPS), 18 avenue Edouard Belin, F-31401 Toulouse Cedex 9, France. Tel.: +33 561 55 85 84.

E-mail addresses: mcgonzal@uv.es (M.C. González-Sanpedro), moreno@uv.es (J. Moreno), evamaria.rubio@uclm.es (E. Rubio).

¹ Tel.: +33 561 55 85 84.

² Tel.: +34 96 3543112.

³ Tel.: +34 96 7599200.

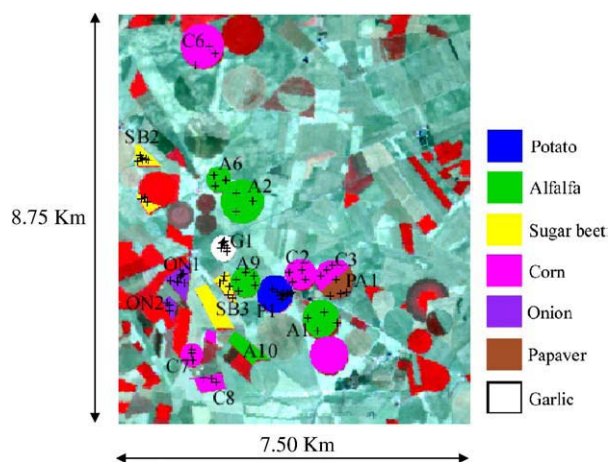


Fig. 1. Landsat false colour (15 July 2003) close-up of “Las Tiesas” experimental facilities site with the location of the monitored fields (highlighted in colours) and the points where individual samples were measured.

photosynthesis and biogenic emissions. For instance, in irrigation management, LAI is required to model the surface resistance when calculating evapotranspiration (ET) by direct application of the Penman–Monteith’s equation (Allen, 2000). ET models based on surface energy balance and hydrological models that take into account the role of vegetation also require LAI as input for partitioning ET into evaporation and transpiration (Montaldo & Albertson, 2003; Norman et al., 1995; see also Hadria et al., 2006).

In crop monitoring studies conducted in recent years in the region of Barrax, Spain (Berger et al., 2000; Moreno et al., 2004), in-situ LAI measurements have been performed during specific remote sensing experiments and can be used to calibrate crop growth models and coupled vegetation and hydrological models. However, given the large number of crop types, the large differences in crop calendar and the diversity of field management in the region, in-situ LAI measurements appeared insufficient as they are usually available for only a limited number of fields and dates.

Multitemporal high resolution optical remote sensing is considered an advantageous alternative to infer both spatial and

temporal LAI, provided that the retrieval of LAI from satellite data is effective for the diversity of crop types in the region.

Methodologies to derive LAI from satellite optical data have been the subject of a large amount of work. In contrast, few papers have addressed the effective model inversion of high resolution satellite images for a complete temporal series of data for various crop types in a given region. The crop types present in the region of Barrax include: cereals, corn, alfalfa, sugar beet, onion, garlic, papaver. Some of the crop types (onion, garlic, papaver) have not been addressed in previous studies.

In the present study, we focused on the assessment of a LAI model inversion approach applied to multitemporal optical data over the region of Barrax. Both the inversion approach and data sources are chosen because of their wide use: the inversion makes use of the PROSPECT+SAIL model and the satellite data are Landsat images. First, the PROSPECT+SAIL model benefits from in-situ measurements of crop biophysical properties used as constraints on the model parameters; second, we use a model inversion technique consisting of a Look Up Table to invert a complete time series of Landsat-TM and ETM+ scenes acquired all along the crop growth period in the Barrax area (i.e. from March to September). The image data used here consisted of twelve Landsat-TM and ETM+ scenes. Our objective is to obtain temporal LAI curves for the diversity of crops in the area of Barrax.

The paper is organised as follows: first, the study area, ground measurements and satellite dataset used in this work are described. Second, the methodology is detailed including a review of models and inversion approaches, which results in the choice of the retained model and approach. The methodology itself, which includes the derivation of a land use map and an inversion of the selected model, is described. Finally results and validation are presented followed by a discussion.

2. Site description and datasets

2.1. Site description

The area of Barrax (Castilla-La Mancha, Albacete, Spain) is located on a central plateau at 700 m above sea level. Relevant

Table 1

Mean and standard deviation values of the Leaf Dry Matter (DM), Leaf Water Content (WC), Chlorophyll content (CC) and Fraction of Vegetation Cover (FVC) measured during the field campaigns for each crop

Crop	Dry matter (DM) (g m ⁻²)	Water content (WC) (g m ⁻²)	Chlorophyll content CC) (μg cm ⁻²)	Fraction of vegetation cover (FVC)
Corn	61±6	180±18	50.6±0.8	0.63±0.08
Potato	43±3	223±21	35.6±0.5	0.96±0.04
Sugar beet	72±11	400±120	44.3±1.4	0.94±0.02
Garlic	130±30	600±140	15±2	0.12±0.09
Onion	83±7	680±150	20±2	0.64±0.05
Alfalfa	89±23	140±70	48.5±1.2	0.59±0.04
Alfalfa	65±19	130±50	48.5±1.2	0.59±0.04
Sunflower	77±5	390±50	42.7±0.4	0.16±0.05
Vine	90±10	190±30	34.6±0.7	NA

Data correspond to the SPARC-2003 campaign except for sunflower and vine that were measured in SPARC-2004 campaign. Chlorophyll content and FVC of alfalfa fields was assigned the same as it was measured only once.

Table 2
Mean LAI-2000 measurements during the SPARC-2003 for each measured field

CROP/ID		LAI
Alfalfa	A9	2.99±0.16
Alfalfa	A1	1.36±0.13
Alfalfa	A10	1.90±0.08
Potato	P1	5.4±0.4
Onion	ON1	2.3±0.4
Sugar beet	SB3	4.1±0.7
Corn	C2	3.5±0.4
Corn	C1	3.3±0.4
Garlic	G1	0.56±0.10

Spatial distribution of the measurements is shown in Fig. 1.

characteristics of this region are its flat topography and the presence of large uniform land use units. Castilla-La Mancha is one of the driest regions of Europe with mean annual precipitation of about 400 mm, which is mostly concentrated in spring and autumn. The study site covers an area of 51 km×38 km. Vegetation in this site is representative of the crop types and agricultural practices of Castilla-La Mancha. Two thirds of the study area is dry land with dominant winter/spring cereals (60%) and bare soil/fallow land (30%), and the rest is irrigated land cropped with corn, wheat, barley, sunflower, alfalfa, onion and vegetables.

2.2. Ground biophysical measurements

Biophysical parameters and ground information used in this work were collected in the 2003 growing season in the framework of two different activities: the experimental campaigns of ESA/SPARC-2003 (Moreno et al., 2004), and the field activities planned in the DEMETER project (Jochum & Calera, 2006).

Intensive field measurements of biophysical properties were collected during the period 11–15 July 2003. These measurements were concentrated in a 10 km×10 km site within the “Las Tiesas” experimental facilities of the Diputación Provincial de Albacete. The measured biophysical parameters comprised the following: LAI, Leaf Chlorophyll content CC, Leaf Water Content WC and Leaf Dry Matter DM. The measurements were taken in fields of alfalfa (*Medicago sativa* L.), corn (*Zea mays* L.), garlic (*Allium sativum* L.), onion (*Allium cepa* L.), papaver (*Papaver somniferum* L.), potato (*Solanum tuberosum* L.) and sugar beet (*Beta vulgaris* L.). The Leaf Chlorophyll Content was measured using the CCM-200 Chlorophyll Content Meter, which was calibrated through laboratory analysis of specific samples (Gandía et al., 2004). Leaf Water Content and Leaf Dry Matter were determined by weighing the wet and dry samples and by estimating the leaf area through the analysis of digital pictures. LAI measurements were made using the Plant Canopy Analyser, LAI-2000 (LI-COR Inc., Lincoln, NE, USA). LAI measurements were carried out under uniform clear diffuse skies at low solar elevation to prevent the effects of direct sunlight on the sensor. Fig. 1 shows a Landsat close-up of the “Las Tiesas” site with the measured fields highlighted in colour, and the location of the individual samples that were collected. In

this figure, the circular fields have diameters that range between 300 m and almost 2 km. These circular fields correspond to irrigation units known as “pivot”. The figure shows that a large part of the image is not covered by vegetation at the date of 15 July. The non-vegetated areas include mainly harvested cereal fields with variable reflectances, whereas bare soil surfaces have higher reflectance. The nomenclature chosen in this paper for the fields is F_n , where F is a letter denoting the field type (A stands for Alfalfa, C for Corn, G for Garlic, ON for Onion, P for Potato, PA for Papaver and SB for Sugar Beet) and n is a digit corresponding to the field number. For consistency with other analyses using the same datasets (Moreno et al., 2004), the numbering of the fields from the original dataset is maintained. Table 1 lists the mean and standard deviation values of DM, WC, CC and Fraction of Vegetation Cover (FVC) measured for each crop. LAI measurements for each individual field are given in Table 2. Here, an average value was calculated for each individual field from the sets of measurements performed on the various samples measured within every given field. For a more detailed description of the ground dataset of the SPARC-2003 campaign, see Moreno et al. (2004). The different parameters in Tables 1 and 2 were found weakly correlated (with r^2 of the order of $r^2 \sim 0.25$), except LAI and Dry Matter Content ($r^2 \sim 0.5$) (Fernández et al., 2004). In particular, for the same Fraction of Vegetation Cover, e.g. 0.6 for corn, onion and alfalfa in Table 1, additional information is contained in LAI, e.g. LAI values range from 1.4 to 3.5 in Table 2. Phenology observations (e.g. on potato and onion) made by the Irrigation Advisory Service (IAS) of ITAP (Instituto Técnico Agronómico Provincial) were also available.

2.3. Remote sensing data

Table 3 lists the twelve Landsat 5 and 7 images acquisition dates and the illumination geometries. Pre-processing of the Landsat images comprised first their geo-coding, then calibration and finally the atmospheric correction providing surface reflectance images. The geo-coding of the twelve images was

Table 3

List of Landsat-7 & Landsat-5 data acquisitions, solar zenith angle (degrees) at satellite pass time and solar zenith angle (degrees) used as input of SAIL for generating the LUTs

Date	DOY	Satellite	Solar zenith	Solar zenith used in the LUT	LUT reference
10/03	69	Landsat-7	49.20	49.00	1
27/04	117	Landsat-7	32.05	32.00	2
20/05	140	Landsat-7	26.97	27.00	3
29/05	149	Landsat-7	25.88	27.00	3
29/06	180	Landsat-5	28.00	29.00	4
08/07	189	Landsat-5	29.00	29.00	4
15/07	196	Landsat-5	29.00	29.00	4
24/07	205	Landsat-5	31.00	32.00	5
31/07	212	Landsat-5	32.00	32.00	5
09/08	221	Landsat-5	33.00	32.00	5
25/08	237	Landsat-5	37.00	37.00	6
17/09	260	Landsat-5	42.72	43.00	7

A total number of 7 Look Up Tables were generated (for each crop).

performed by using a total of more than 100 ground control points (GCPs) distributed over the Landsat scenes and measured in-situ with GPS. The images were first rectified using a polynomial transformation with an error lower than 1 pixel, and then resampled at 30 m spatial resolution by using the nearest neighbour algorithm. The images were subsequently calibrated by calculating the at-sensor radiance, and the surface reflectances were retrieved by performing the atmospheric correction following [Guanter et al. \(2007\)](#). In this step, the atmosphere is considered invariant across 30×30 km windows, while the surface reflectance is allowed to vary from pixel to pixel, and it is assumed to be represented as a linear combination of two vegetation and soil endmembers. An inversion of the top of atmosphere (TOA) radiances in 5 reference pixels is performed to obtain aerosol optical thickness (AOT), water vapor and the proportions of vegetation and soil in the 5 pixels. The estimated atmospheric component concentrations are then used to convert the TOA radiances to surface reflectances. This atmospheric correction method has been validated with MERIS and sun-photometer data ([Guanter et al., 2007](#)).

3. Methodology

3.1. Land use map

The time series of Landsat images was first used to generate a land use map of the area. The classification method was based on a multitemporal supervised algorithm that takes advantage of the different phenological development of the crops in the area. The resulting classification has eleven general classes initially

defined for irrigation management purposes. Apart from urban areas and water/wet areas, the land use and land cover classes include: Natural vegetation, Spring irrigated crops (mostly small grain cereals), Summer irrigated crops (mostly corn and sugar beet, locally other crops), Double harvest (cereals in spring followed by irrigated summer crops), Alfalfa, Fallow/Bare Soil (in this area fallow is equivalent to bare soil), Dry crops (mainly non-irrigated cereals), Other crops (unknown), Vineyard (*Vitis vinifera* Lin.)/Fruit trees. The validation was done with 519 plots. The Kappa coefficient, K , which is an indicator of the overall accuracy of the classification was $K=0.92$. The producer's accuracy is respectively of 80% for Natural Vegetation, 100% for Spring irrigated crops, 98% for Summer irrigated crops, 79% for Double harvest, 100% for Alfalfa, 100% for Fallow/Bare Soil, 88% for Dry crops and 83% for Vineyard. A further classification step has been done, based on more detailed information that was available for some fields through field survey, to partition the land use/land cover classes into crop types. This information was overlaid to the general classification giving refined classes for corn, sugar beet, wheat (*Triticum* L.), barley (*Hordeum vulgare* L.), onion, garlic, sunflower (*Helianthus annuus* L.), peas (*Pisum sativum* L.), potatoes, oat (*Avena sativa* L.), pepper (*Capsicum annuum*), ryegrass (*Lolium* L.), kenaf (*Hibiscus cannabinus* L.) and papaver fields. [Fig. 2](#) shows the final land use map of the study area. Therefore, the classification of [Fig. 2](#) contains general classes (class 1 to class 11) and detail classes for a subset of fields (class 12 to class 21). For purposes of LAI retrieval, some categories such as Urban areas, Water/wet areas and Fallow fields, were masked in the Landsat images prior to inversion.

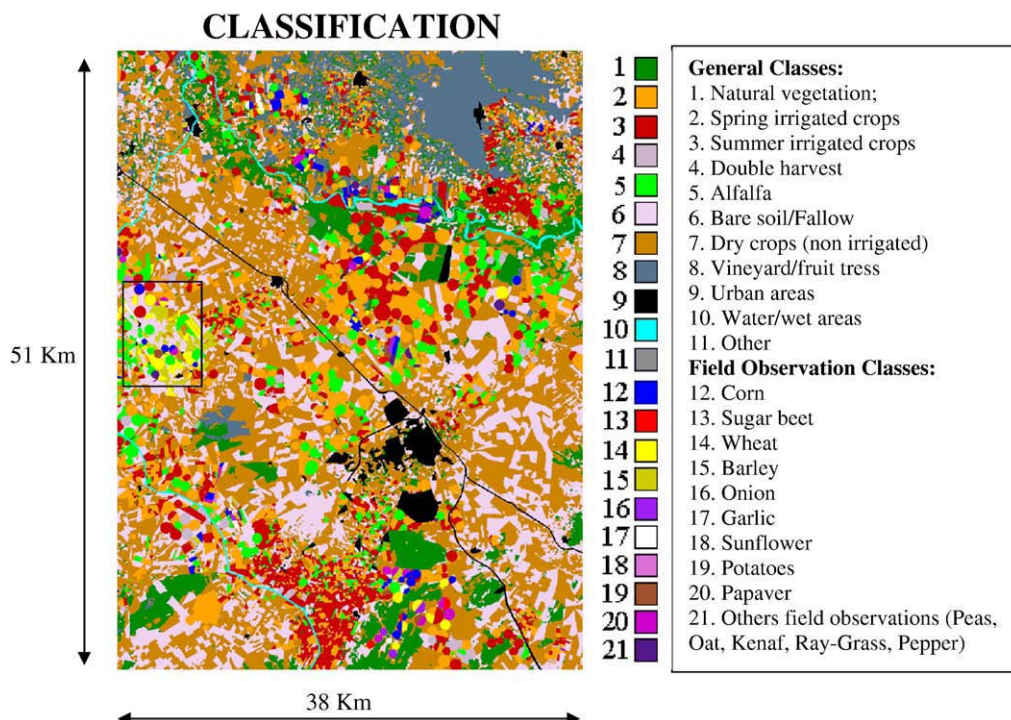


Fig. 2. Land use map of the study area. Classes 12 to 21 are local refinements of classes 2 to 7. The black rectangle corresponds to [Fig. 1](#).

Table 4
Range of values and number of values inside this range (*i*) that have been used in the Landsat Look Up Table generation for each crop on June the 29th, July the 8th and July the 15th

	<i>N</i>	CC ($\mu\text{g cm}^{-2}$)	WC (g m^{-2})	DM (g m^{-2})	LAI	<i>a</i>	<i>b</i>	<i>h</i>
Corn	1.6	50.0	[100, 200] <i>i</i> =3	[50, 70] <i>i</i> =3	[0.1, 6.0] <i>i</i> =60	[−0.4, −0.6] <i>i</i> =3	−0.4	[0.1, 0.3] <i>i</i> =5
Sugar beet	1.6	44.0	[300, 600] <i>i</i> =4	[50, 80] <i>i</i> =7	[0.1, 6.0] <i>i</i> =60	[−0.2, 0.0] <i>i</i> =3	0.8	[0.3, 0.6] <i>i</i> =7
Potato	1.6	36.0	[200, 300] <i>i</i> =3	[40, 50] <i>i</i> =3	[0.1, 6.0] <i>i</i> =60	Spherical		[0.1, 0.2] <i>i</i> =3
Sunflower	1.6	43.0	[300, 600] <i>i</i> =7	[60, 90] <i>i</i> =7	[0.1, 6.0] <i>i</i> =60	[0.7, 0.9] <i>i</i> =3	0.0	[0.1, 0.25] <i>i</i> =4
Alfalfa	1.7	49.0	[120, 160] <i>i</i> =5	[30, 80] <i>i</i> =6	[0.1, 6.0] <i>i</i> =60	[0.8, 1.0] <i>i</i> =3	0.0	[0.05, 0.12] <i>i</i> =8
Garlic	1.6	15.0	[500, 700] <i>i</i> =5	[50, 200] <i>i</i> =4	[0.1, 6.0] <i>i</i> =60	[−0.1, 0.1] <i>i</i> =3	0.5	[0.05, 0.07] <i>i</i> =3
Onion	1.6	20.0	[500, 800] <i>i</i> =4	[50, 90] <i>i</i> =5	[0.1, 6.0] <i>i</i> =60	[−0.1, 0.1] <i>i</i> =3	0.5	[0.05, 0.07] <i>i</i> =3
Natural vegetation	1.5	[20.0, 50.0] <i>i</i> =4	[50, 200] <i>i</i> =4	[10, 90] <i>i</i> =5	[0.1, 6.0] <i>i</i> =60	Spherical		[0.05, 0.15] <i>i</i> =3
Vineyard–fruit trees	1.6	36.0	[150, 250] <i>i</i> =3	[80, 100] <i>i</i> =3	[0.1, 2.5] <i>i</i> =25	Spherical		[0.08, 0.12] <i>i</i> =5
Others	1.6	[10.0, 50.0] <i>i</i> =5	[100, 800] <i>i</i> =8	[40, 200] <i>i</i> =17	[0.1, 6.0] <i>i</i> =60	Spherical		[0.01, 0.10] <i>i</i> =10

3.2. Retrieval of LAI

This section presents a short review of the LAI retrieval methods and explains the choice of the approach to be used in this work. Secondly, the approach itself is described.

3.2.1. Review of literature

In recent decades, a large amount of work has been published on the derivation of LAI and other biophysical parameters (e.g. fraction of photosynthetically active radiation, chlorophyll content and water content) from optical data. Two main

approaches have been used: empirical and physically-based approaches.

Empirical approaches are based on the experimental relationships between combinations of reflectances in different spectral bands (indices) and the parameter to be retrieved. This approach has been frequently applied to various satellite data to calculate the LAI of large classes or categories of vegetation. In particular, [Turner et al. \(1999\)](#) used Landsat data with empirical relationships to derive the LAI of grassland, shrubland, hardwood and coniferous forest; [Chen et al. \(2002\)](#) used AVHRR, SPOT VGT and Landsat data to retrieve the LAI of

Table 5
Range of values and number of values inside this range (*i*) that have been used in the Landsat Look Up Table generation for each crop for dates others than June the 29th, July the 8th and July the 15th

	<i>N</i>	CC ($\mu\text{g cm}^{-2}$)	WC (g m^{-2})	DM (g m^{-2})	LAI	<i>a</i>	<i>b</i>	<i>h</i>
Corn ^a	1.6 ^b	[35, 60] ^c <i>i</i> =6	[100, 200] <i>i</i> =3	[50, 70] <i>i</i> =3	[0.1, 6.0] <i>i</i> =60	[−0.4, −0.6] ^b <i>i</i> =3	−0.4	[0.1, 0.3] ^{d, e, f} <i>i</i> =5
Sugar beet ^a	1.6	[40, 50] <i>i</i> =3	[300, 600] ^g <i>i</i> =4	[50, 80] <i>i</i> =7	[0.1, 6.0] <i>i</i> =60	[−0.2, 0.0] ^h <i>i</i> =3	0.8	[0.3, 0.6] ⁱ <i>i</i> =7
Potato ^a	1.6	[25, 45] <i>i</i> =5	[200, 300] <i>i</i> =3	[40, 50] <i>i</i> =3	[0.1, 6.0] <i>i</i> =60	Spherical		[0.1, 0.2] <i>i</i> =3
Sunflower ^a	1.6	[38, 48] <i>i</i> =3	[300, 600] <i>i</i> =7	[60, 90] <i>i</i> =7	[0.1, 6.0] <i>i</i> =60	[0.7, 0.9] <i>i</i> =3	0.0	[0.10, 0.25] <i>i</i> =4
Alfalfa	1.7	[45, 55] <i>i</i> =3	[120, 160] <i>i</i> =5	[30, 80] <i>i</i> =6	[0.1, 6.0] ^j <i>i</i> =60	[0.8, 1] <i>i</i> =3	0.0	[0.05, 0.12] <i>i</i> =8
Garlic ^a	1.6	[15, 55] <i>i</i> =3	[500, 700] <i>i</i> =5	[50, 200] <i>i</i> =4	[0.1, 6.0] <i>i</i> =60	[−0.1, 0.1] <i>i</i> =3	0.5	[0.05, 0.07] <i>i</i> =3
Onion ^a	1.6	[10, 20] <i>i</i> =3	[500, 800] <i>i</i> =4	[50, 90] <i>i</i> =5	[0.1, 6.0] <i>i</i> =60	[−0.1, 0.1] <i>i</i> =3	0.5	[0.05, 0.07] <i>i</i> =3
Natural vegetation	1.5	[20, 50] <i>i</i> =4	[50, 200] ^k <i>i</i> =4	[10, 90] ^k <i>i</i> =5	[0.1, 6.0] <i>i</i> =60	Spherical ^{l, m}		[0.05, 0.15] <i>i</i> =3
Vineyard–fruit trees	1.6	[25, 45] <i>i</i> =5	[150, 250] ⁿ <i>i</i> =3	[80, 100] <i>i</i> =3	[0.1, 2.5] <i>i</i> =25	Spherical		[0.08, 0.12] <i>i</i> =5
Others	1.6	[10.0, 50.0] <i>i</i> =5	[100, 800] <i>i</i> =8	[40, 200] <i>i</i> =17	[0.1, 6.0] <i>i</i> =60	Spherical		[0.01, 0.10] <i>i</i> =10
Wheat, barley ^o	1.6	[5, 50] ^p <i>i</i> =10	[100, 500] <i>i</i> =5	[40, 60] ^q <i>i</i> =3	[0.1, 6.0] <i>i</i> =60	[−0.3, 0.3] <i>i</i> =7	−0.4	[0.01, 0.03] ^f <i>i</i> =3

^a Applied from June the 29th to September the 17th.

^b Koetz et al., 2005.

^c Viña et al., 2004.

^d Qin et al., 2002.

^e España et al., 1999.

^f Combal et al., 2002b.

^g Combal et al., 2002a.

^h Duke & Guérif, 1998.

ⁱ Andrieu et al., 1997.

^j Confalonieri & Bechini, 2004.

^k Weiss & Baret, 1999.

^l Fang et al., 2003.

^m Fang & Liang, 2003.

ⁿ Fourty, 1996.

^o Applied from March the 10th to May the 29th.

^p Kneubühler, 2002.

^q Verhoef & Bach, 2003.

forests and crops. In a similar way, this approach was applied to particular crop types, such as wheat, with Landsat-TM data (Duchemin et al., 2006) and with SPOT HRV data (Clevers et al., 2002 among others).

A drawback is that the general applicability of these empirical approaches is reduced because the vegetation indices (VI) are affected by many factors including atmospheric effects, leaf structure, canopy geometry, vegetation developmental stage, geometry of observation, understory vegetation and soil conditions (Baret & Guyot, 1991; Boegh et al., 2002; Gitelson et al., 2005; Turner et al., 1999).

Physically-based approaches (e. g. Kimes et al., 2000) are based on the application of Radiative Transfer models. These models describe the physical processes of radiative transfer in the soil vegetation system, connecting the canopy biophysical variables and the canopy reflectance. These approaches, though more complex, are more general in application because they can account for the different sources of variability, although in many cases the information needed to constrain model inputs is not available.

For the objective of this study, which is to investigate the applicability and accuracy of LAI inversion over a complex agricultural landscape, we retain a physically-based approach, taking the benefit of having experimental data to be used as model constraints. Nevertheless, we will compare the results from a physically-based approach to those obtained using an empirical approach.

Among physically-based approaches, the most widely used consists of the inversion of a simple canopy radiative transfer model coupled with a leaf model. Examples of canopy models are: SAIL (Verhoef, 1984), Kuusk (Kuusk, 1995; Nilson & Kuusk, 1989) and NADI (Gobron et al., 1997). Well-known leaf models are PROSPECT (Jacquemoud & Baret, 1990), LIBERTY (Dawson et al., 1998), and LEAFMOD (Ganapol et al., 1999). Regarding inversion techniques different approaches have been used: a) direct numerical inversion (Bicheron & Leroy, 1999; Gao & Lesht, 1997), b) Look Up Tables (Combal et al., 2002a; Weiss et al., 2000), c) neural network techniques (Fang & Liang, 2003; Qi et al., 2000; Weiss & Baret, 1999 and d) genetic algorithms (Fang et al., 2003).

Among the available models and inversion techniques, we retained models which have been widely applied and an inversion technique which is easy to implement: the model is PROSPECT+SAIL and the inversion is based on Look Up Tables (LUTs).

Table 6

Average soil spectrum reflectance and standard deviation in the image of July the 15th and the HyMAP soil spectrum used in the LUTs filtered to the LANDSAT bands for comparison

Landsat bands	Landsat	HyMAP filtered reflectance
B1	0.12±0.03	0.07
B2	0.20±0.04	0.17
B3	0.27±0.05	0.25
B4	0.37±0.06	0.31
B5	0.48±0.06	0.49
B7	0.42±0.07	0.38

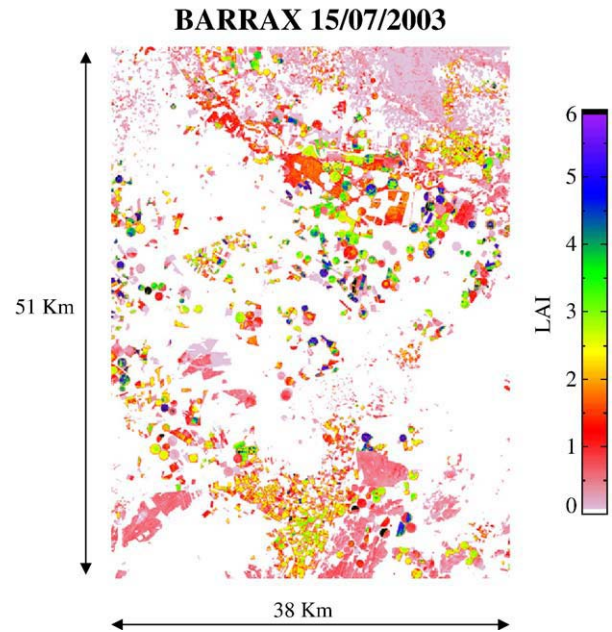


Fig. 3. Landsat derived LAI map in July the 15th, showing contrast between crops.

3.2.2. PROSPECT and SAIL models

In this study, we used the ‘4 inputs’ version of the PROSPECT model, PROSPECT v. 3.01 (5 May 1998), available from http://www.sigu7.jussieu.fr/Led/LED_prospect_e.htm. This 4 inputs model version has been widely used in the literature: for instance Jacquemoud & Baret, 1990; Haboudane et al., 2004. The model was calibrated with the LOPEX dataset (Hosgood et al., 1995; Jacquemoud et al., 1996).

The PROSPECT model simulates the reflectance and transmittance of a leaf in the region from 400 to 2500 nm. The model assumes that the leaf is a stack of N elementary layers separated by $N-1$ air spaces, and that the biochemical components are mixed homogeneously in the leaf. The absorption coefficient of the leaf $k(\lambda)$ is then given by the following equation:

$$k(\lambda) = k_0(\lambda) + \sum_i \frac{C_i k_i(\lambda)}{N} \quad (1)$$

where, N is the structural mesophyll parameter, λ is the wavelength, C_i the concentration of the constituent, k_i the specific absorption coefficient of the constituent and k_0 the absorption of an albino leaf under 500 nm. The specific absorption coefficient of each constituent can be determined by calibrating the model.

There is also a 5 inputs version of PROSPECT model that includes the so-called brown pigments or senescent pigments concentration (Demarez et al., 1999; Zhang et al., 2005). However this version of the model has not benefit from such a extensive calibration.

The SAIL version available for this study is the 4SAIL developed by Verhoef (unpublished), available for the Fluor-Mod project (Miller et al., 2004). A version of FluorMod is

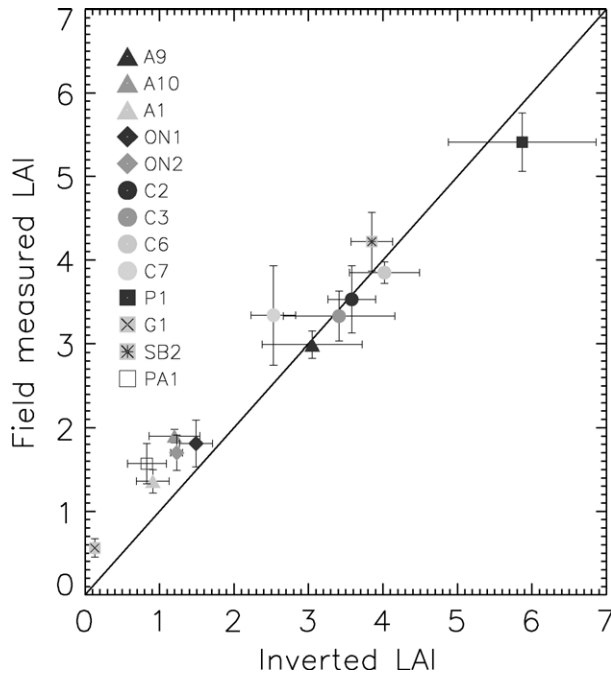


Fig. 4. Validation of Landsat derived LAI with LAI-2000 measurements. A stands for Alfalfa, C for Corn, G for Garlic, ON for Onion, P for Potato, PA for Papaver and SB for Sugar Beet.

available from: <http://www.ias.csic.es/fluormod/>. 4SAIL is a version of the original SAIL model (Verhoef, 1984), which includes the hot spot effect and has been improved numerically and computationally with respect to previous versions.

Inputs to the PROSPECT model are Leaf Chlorophyll Content (CC), Leaf Water Content (CW), Leaf Dry Matter Content (DM) and the Leaf Structural Parameter, N . Inputs to the SAIL model are structural parameters that include LAI, a , and b , two parameters that describe the Leaf Angle Distribution (LAD), as explained in Verhoef, 2002, the Hot Spot parameter, h , the background soil spectrum and the geometry of observation. Both, parameter a and parameter b can vary between -1 and 1 , but the sum of their absolute values has to be always less than or equal to 1 . Parameter a controls the average leaf inclination angle (ALA), which in the SAIL model can range from 8.52° ($a=1$) to 81.48° ($a=-1$). Parameter b characterises the bimodality of the LAD. High values of b correspond to a high frequency of both horizontal and vertical leaves (Verhoef, 2002).

3.2.3. Chosen inversion approach

Even in the case of simple radiative transfer models, the estimation of LAI through inversion of reflectance data is an ill-posed problem, as the number of unknown parameters is higher than the spectral information. The problem can be solved by using a-priori information (Combal et al., 2002b), for instance using in-situ measurements to limit the range of parameters values. Thus, taking advantage of the vegetation biophysical measurements that were acquired for our study area, the more general physically-based approach has been preferred to a semi-empirical approach.

In a probabilistic description of the inverse problem (Tarantola, 2005), the cost function f describing the discrepancies between the simulations and the measurements will be proportional to the term:

$$f \propto (\vec{\rho}^{\text{LANDSAT}} - \vec{\rho}^{\text{LUT}})^T C^{-1} (\vec{\rho}^{\text{LANDSAT}} - \vec{\rho}^{\text{LUT}}) \quad (2)$$

where, C , is the covariance matrix of the measurements accounting for measurement errors. The elements off-diagonal are not null when errors are correlated between bands. Usually, correlations are unknown, and a first approximation to the problem consists in neglecting them. The inversion of our Look Up Tables consisted in finding which spectrum from the Look Up Table minimizes the following expression:

$$K = \sum_{b=1}^6 (\rho_b^{\text{LANDSAT}} - \rho_b^{\text{LUT}})^2 \quad (3)$$

The later equation implies that measurement errors are assumed equal (as the same weight has been given to all bands) and without correlations (elements off-diagonal are zero).

Due to the lack of information to quantify the covariance matrix, it has been chosen to give the same weight to all bands. Moreover, in this sort of methodology, measured reflectances are compared with “ideal” simulated reflectances, as it is assumed that the model has no errors. Errors in the model are indeed very difficult to quantify, also they may be comparable or even higher than measurements errors.

The inversion following Eq. (3) is applied to each of the Landsat images, on a pixel by pixel basis, for each specific crop type according to the land use map (see Fig. 2).

The inversion method consists in using crop-specific Look Up Tables (LUTs) which have been created using the outputs of PROSPECT+SAIL models. The PROSPECT model computes the leaf reflectance and transmittance needed for running the SAIL model.

Both PROSPECT and SAIL models were run by steps of 2.5 nm wavelength. To simulate Landsat-like spectra, the SAIL model was run in the range from 400 to 2500 nm. The atmospheric parameters needed for this version of SAIL (extraterrestrial solar irradiance, direct solar transmittance, atmospheric spherical albedo and diffuse solar transmittance) were calculated in the full range from 400 nm to 2500 nm using MODTRAN-4. The 2.5 nm step simulated hyperspectral reflectance is then aggregated using Landsat sensor filters to give a 6 bands spectrum. Look Up Tables adapted to solar zenith angle for each Landsat date (see Table 3) were generated for alfalfa, corn, garlic, onion, sugar beet, potato, sunflower, vineyard/fruit trees, wheat/barley and natural vegetation. In addition, a general LUT was created for the rest of crops (peas, pepper, etc).

Inputs to the PROSPECT+SAIL models are experimental data, when available, completed by information from literature. The structural parameters a and b are established based on our knowledge of the plant structure (erectophile, planophile, extremophile ...) and the related LAD parameterisation values in SAIL. Tables 4 and 5 list these parameters and their ranges of values. In a first approximation, the ranges of values centered on in-situ measurements collected in July 2003 (and also in July

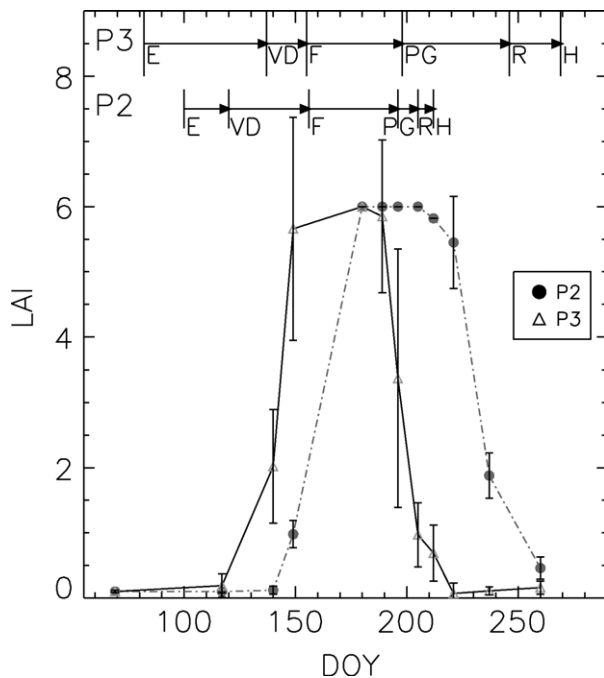


Fig. 5. Retrieved LAI for two potato fields (P2 and P3) with different calendar. Phenological observations are indicated on top. P2 has a longer cycle than P3: emergence is earlier and harvest is later than for P2. E stands for Emergence, VD for Vegetation Development, F for Flowering, PG for Potato Growing, R for Ripening and H for Harvest.

2004) were applied to the whole season assuming that the ranges measured at these dates are sufficiently large to cover all plausible values. One exception concerns chlorophyll content, which commonly varies within the plant cycle. The distribution of chlorophyll has been widened for dates other than June 29 to July 15. To run the models, we choose to give discrete values within the interval with a regular step. The exact number of steps used for each crop is indicated in Tables 4 and 5. Typical values in the LUT are at $5 \mu\text{g cm}^{-2}$ steps for CC; 100 mg m^{-2} for CW; 10 mg cm^{-2} for DM; and 0.1 steps for a , h and LAI. The LAI range is between 0.1 and 6.0 for all crops except for vineyards which varies from 0.1 to 2.5. Vineyard in the region has low fractional cover (<5%), (Lanjeri et al., 2001) and low LAI. For the LAD parameter b , and the leaf structural parameter N , a unique value was given for each crop type, as it is frequently done in literature (e.g., Combal et al., 2002a; Jacquemoud et al., 1995; Haboudane et al., 2004).

We use as input to SAIL, the soil spectrum extracted from a HyMAP airborne hyperspectral sensor image at nadir, acquired simultaneously to the SPARC campaign in Barrax, in July 2003. The spectrum has been chosen to have finer spectral resolution than Landsat: 2.5 nm wavelength resolution interpolated from the original spectrum. The HyMAP spectrum is found very close to the mean spectrum derived from bare soil/fallow class in the Landsat July image (Table 6). We use a fixed soil spectrum in the SAIL model, because the Barrax study site is a dry area, with low variability in soil type. This assumption may not hold for irrigated fields. However, since the evapotranspiration rates are high, we consider that the effect of irrigation is not resilient. The

effect will be important for crops that have been irrigated a few hours prior to the image acquisition, and at low stage development (crops with low FCV).

4. Results and validation

4.1. LAI mapping

A map of LAI was generated for every Landsat image, which are listed in Table 3. Fig. 3 shows the LAI map for July 15. For this date, non-vegetated pixels (bare soil/fallow fields, and already harvested small grain cereal fields) have been masked out. LAI values range from 0.1 to 6. The lowest LAI values (in light pink colour) correspond mainly to vineyards, and the highest LAI values (dark violet and black colour) to summer irrigated crops (sugar beet, corn, potatoes) and alfalfa. The mean value of LAI for vegetated pixels is 1.1, and the standard deviation (STD) is 1.2. The LAI distribution is as follows: 80% of the vegetation pixels have $\text{LAI} < 2$, 16% have a LAI in the range [2–4] and 4% of the pixels have $\text{LAI} > 4$. If we exclude vineyard and natural vegetation, the mean LAI value for crops is $\text{LAI} = 1.8$ with a $\text{STD} = 1.4$, with 59% of the pixels having $\text{LAI} < 2$, 33% in the range [2–4] and 7% having $\text{LAI} > 4$. The low mean value of LAI, and the large LAI range (0.1 to 6) are typical of semi-arid agricultural regions where irrigation allows sustained growth despite a rather dry climate. The twelve LAI images denote a dynamic patchy landscape with high contrasts among three vegetation categories (natural vegetation, spring crops and summer crops) and bare soil surfaces. It can be foreseen that the temporal monitoring of crops in such a region is difficult to be done with low resolution data (e.g. MODIS or MERIS), for which a pixel can contain several fields.

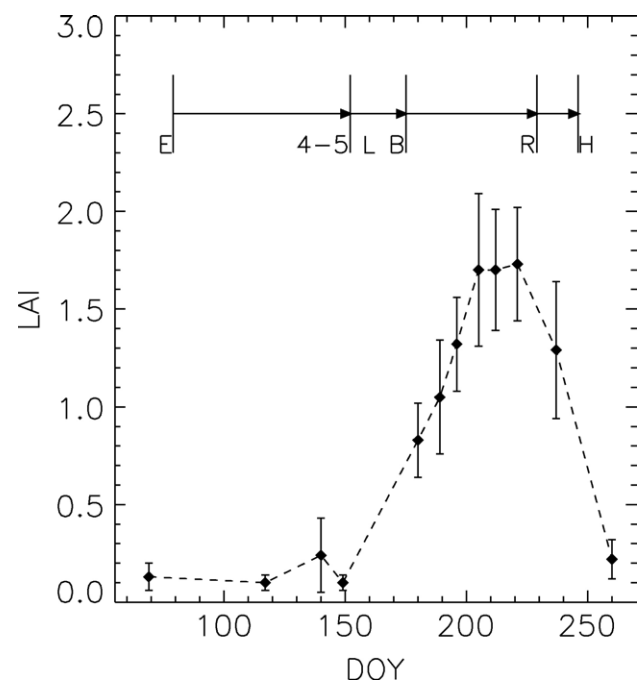


Fig. 6. Retrieved LAI for an onion field. Error bars correspond to the standard deviation for the pixels in the field. Phenological observations for this field are indicated on top: E stands for Emergence, 4–5L for 4–5 leaves, B for bulb growing, R for Ripening and H for Harvest.

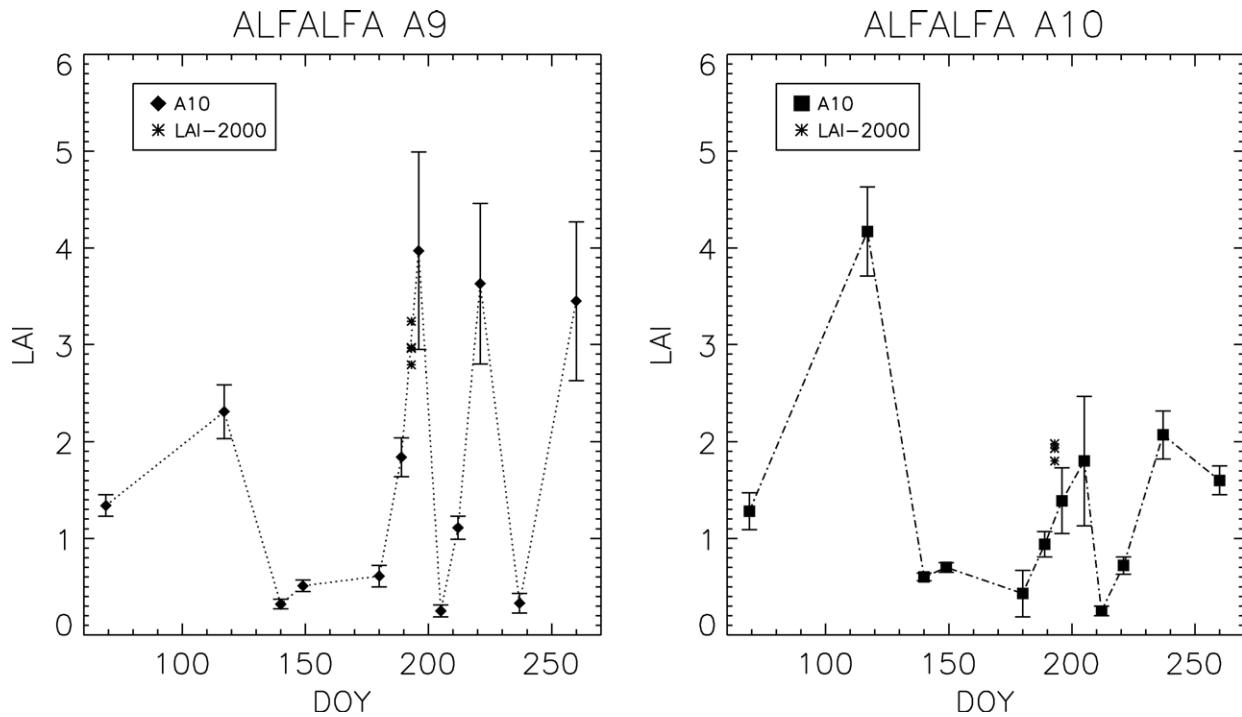


Fig. 7. LAI curves for alfalfa field A9 and field A10. Ground measurements with LAI-2000 instrument are also displayed. Regular cuts of alfalfa are clear. Field A10 had one less cut than field A9 during year 2003.

4.2. Validation using ground data

The LAI values retrieved for July 8 and July 15 were validated against in-situ LAI measurements, which were both averaged over the fields where ground data have been collected (Cf. Fig. 1). Ground measurements were taken during 5 consecutive days (11 to 15 July), thus the retrieved LAI values were interpolated between the two image dates. Fig. 4 presents the comparison for the 13 fields of different crop types. LAI retrieved error bars correspond to the standard deviation of the pixels in the field. Ground data error bars correspond to the standard deviation of the point measurements in each field (around 5).

The comparison shows a high linear correlation ($r^2=0.97$) for the 13 data points of 7 crop types, being: $LAI_{retrieved} = 0.83 * LAI_{observed} + 0.70$. The results do not show any saturation in the whole LAI range (0 to 6), although these results, obtained using only one field with $LAI > 4$ (potato), do not prove that saturation does not exist in the range (4–6). The standard deviation of the inverted LAI ranges from 1% (alfalfa field A2) to 30% (garlic field G1 and papaver field PA1) reflecting field heterogeneity.

A similar agreement is obtained for the July validation when using the LUTs designed for the inversion along the season (larger chlorophyll range).

4.3. LAI temporal monitoring

Temporal curves of the retrieved LAI for different crop types were analysed with respect to their development and phenological stages to assess the performance of the LAI estimations throughout the crop cycles. Figs. 5–10 present examples of

temporal LAI curves for fields of different crop types. When available, the phenology observations and LAI-2000 measurements for the same field are also displayed.

Fig. 5 shows the results for two potato fields with shifted calendars and different cycle length. P2 has a longer cycle than

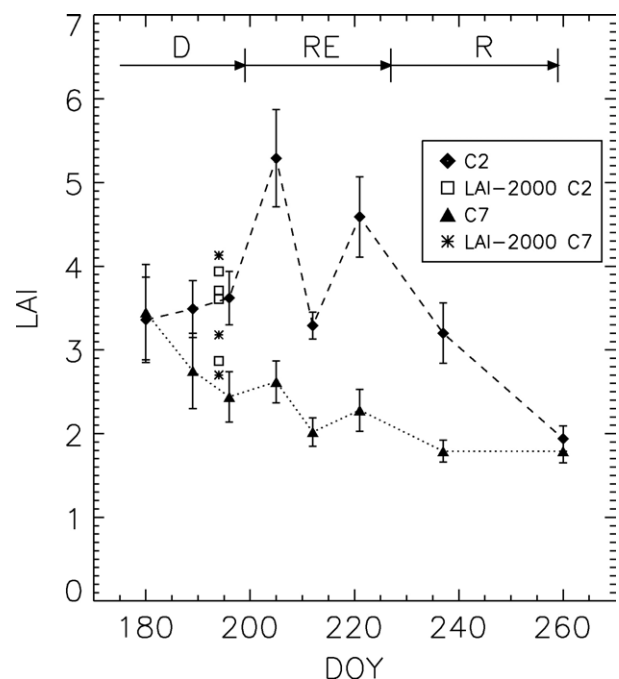


Fig. 8. Retrieved LAI for two corn fields (C2 and C7). The average phenology of corn in the region is indicated on top: D stands for Development, RE for Reproduction and R for Ripening.

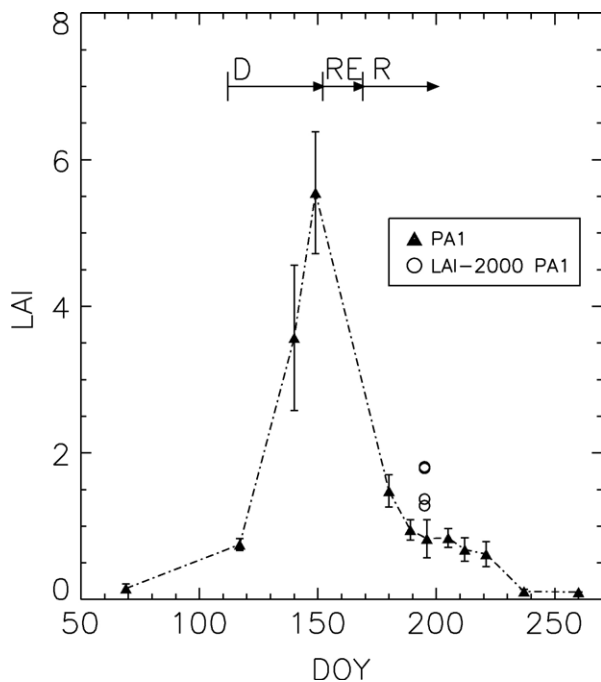


Fig. 9. Retrieved LAI for a papaver field. Phenology for papaver in the region is indicated on top: D stands for development, RE for reproduction and R for Ripening.

P3: emergence is two weeks earlier and harvest is two months later. The retrieved temporal LAI variation follows well the observed phenology. It can also be noted in Fig. 5 that the standard deviation is large during period from flowering to potato growing. This may result from the heterogeneity of the field during this fast varying period.

Fig. 6 shows the temporal LAI curve for an onion field, which also shows consistency with the in-situ observed phenology. Fig. 7 presents the temporal LAI curves for two alfalfa fields. The curves clearly reveal at least two cuts (field A10) and 3 cuts (field A9) between March and September 2003, which are consistent with standard practices in the region.

Fig. 8 presents the temporal curves for two corn fields from June 29 (no Landsat data was available during the first part of the development stage which is from end of May to mid July). The temporal variation does not appear very consistent with respect to the development stage. Field C7 has unexpectedly low LAI for a standard corn crop, but it would be more consistent with a sweet corn which usually has low LAI values in the region. Unfortunately additional ground information that could be used to verify this hypothesis was not available. Field C2 (but also for fields C3 and C6, not presented) has large fluctuations during the reproductive phase, where LAI is expected to be the highest. Similar fluctuations have also been observed with sugar beet fields during the peak period. As a consequence, the inversion for those summer irrigated fields with high LAI will need further studies. Figs. 9 and 10 show the temporal curves for papaver and garlic fields. Although few data have been acquired during the key development stage of the crops, the temporal variation appears smooth. In addition, for these crops with low fractional vegetation cover (onion,

garlic and papaver), the changes in soil conditions (mainly soil moisture) can affect the retrieval results. The smooth behaviour is consistent with the approximation of not considering soil moisture variations in our study area.

In summary, the inversion results shown in Figs. 5–10 indicate the following: a) the results seem correct except for corn and sugar beet, b) the retrieved values are consistent with specific LAI values for each crop; c) the temporal variation of the retrieved LAI is smooth, meaning that the date by date retrieval is consistent.

To better understand these results, we examine the different sources of errors in the methodology. Those include:

a) Radiometric quality of the satellite data (due to absolute miscalibration or temporal radiometric calibration instability, radiometric sensitivity and residual errors after atmospheric corrections). This problem is more important in NIR-SWIR for which temporal instability in the case of Landsat is higher (sinusoidal variation of the calibration coefficients). NIR is the part of the spectra which is the most sensitive to LAI. Crops with high vegetation density, such as corn, require accurate calibration in all bands as LAI retrievals are also affected by total canopy water content. The poor results obtained with corn and sugar beet could be explained by the radiometric quality of the data.

b) Error and uncertainties linked to the a-priori parameters for crop characteristics used in LUT generation. The small retrieval errors as compared to in-situ LAI (Fig. 4) can be explained by the use of in-situ crop parameters measured at the same date to create the LUT. Greater errors are expected for the other dates where input parameters are not measured, as the parameter space is under-sampled.

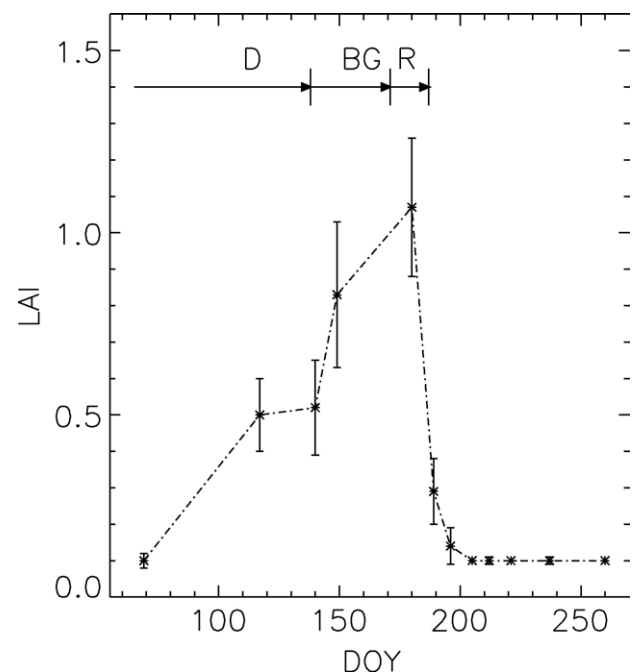


Fig. 10. Retrieved LAI for a garlic field. Phenological observations for this field are indicated on top: D stands for development, BG for bulb growing and R for Ripening.

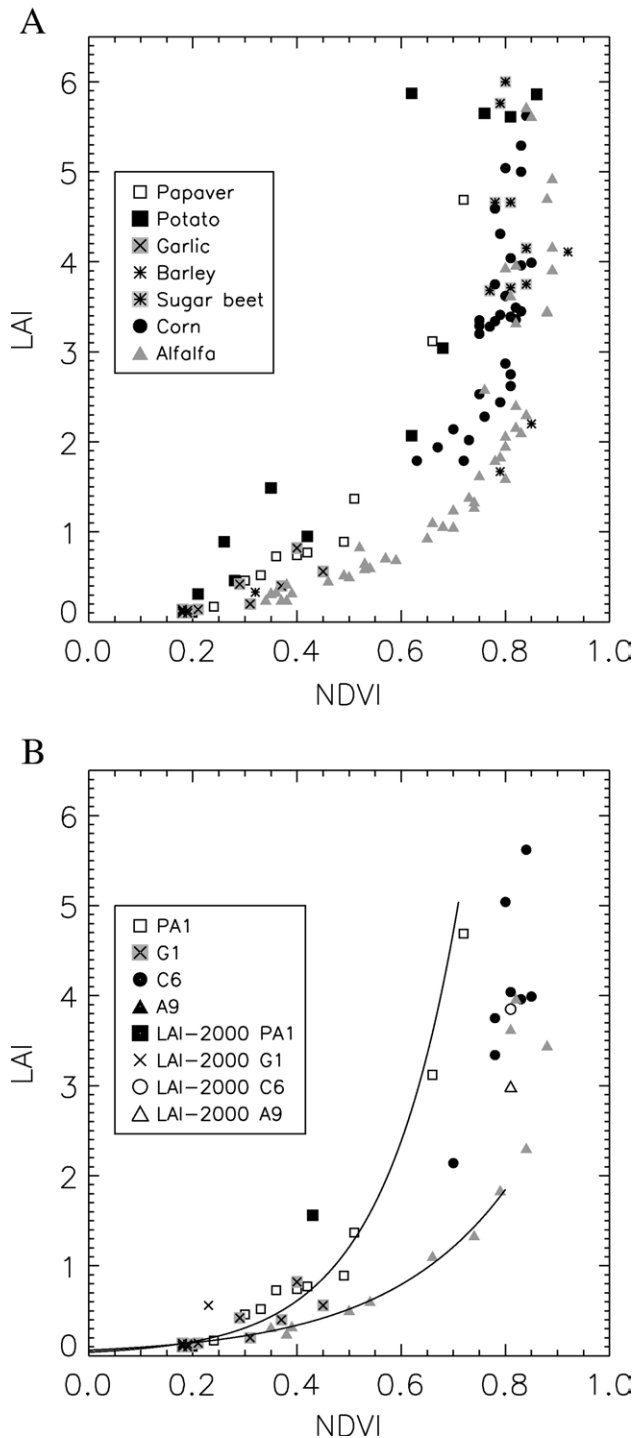


Fig. 11. A) NDVI-LAI relationships for several crops. LAI is the Landsat derived LAI. B) Crop-specific NDVI-LAI relationships derived from model simulations for some crops and in-situ LAI measurements.

c) Limitation of the inversion method. Even though we have reduced the space of possible solutions when constructing the LUTs with a limited range of variation in the parameters, the inversion problem may still be ill-posed. For instance compensation between LAI and other parameters can bias LAI retrievals. This may occur in the inversion for corn and sugar beet. In this study, solutions for individual pixels in a field have

been averaged to reduce the error. Further improvement could be to use the temporal dimension for the search of a better solution, adding a temporal dependent term (a temporal constraint) in the merit function to be minimized. The work of Koetz et al., 2005 showed improvements in corn LAI retrievals when taking into account the temporal dimension by using the phenological LAI dynamics to better define the a-priori information in a refined LUT based inversion method. Other studies also explored the spatial aspects (Atzberger, 2004) and both temporal and spatial dimension (Lauvernet & Baret, 2005).

d) Model limitations. Both PROSPECT and SAIL models apply to “average” vegetation properties, some particularities of crop canopies not being taken into account. For instance a 1-D model like SAIL can not describe accurately structural differences in crops (foliage clumping, row effects). PROSPECT, on the other hand, considers cumulative spectral responses of different leaf pigments (absorbers), which are assumed to be invariable from one leaf to another. This may explain the differences in the results of different crop types. The work by Le Maire et al., 2004, discusses the necessity of re-calibration of PROSPECT. It could be interesting to re-calibrate PROSPECT specifically for agricultural crop leaves or for each crop type in our study at the expense of generality of the method.

e) The specific crop parameters used in the LUTs: the LUT inversion requires knowledge of crop parameters ranges in the area under study. When applying this methodology to other regions, the question is whether these parameters should be adapted locally. In the literature, there is a lack of documentation about the parameters that have been used in the PROSPECT+SAIL models for LAI inversions. In particular, dry matter content is often poorly documented. Surprisingly the largest uncertainties were found in well-studied crops like corn, rather than crops like onion or garlic. For these last crops, a priori parameters are readily different (e.g. large leaf water content) but the inversions are correct. Further field work could help to properly characterize crop parameters and their temporal variation to be used as a-priori in simple RT modelling inversion.

f) Soil variability (soil type and soil moisture). When a single soil spectrum is used, the soil variability caused by soil type or soil irrigation can give errors in the simulated vegetation spectra, propagating to errors in LAI inversion. Simulations show that the effect of soil background is more important for erectophile than for planophile vegetation, at lower fraction cover than at higher fraction cover (not shown). Also, a brighter soil reduces the dynamic range of reflectance in the NIR as a function of LAI. This case is less favourable to LAI inversions. However, as the reflectance variation with LAI is different with the wavelength, it is not clear how this could actually affect the inversions using the full spectra. To quantify the background effect on the inversion, we used two soil spectra, the fixed spectrum used in the LUT multiplied by brightness factor 1.1 and 0.9 ($\pm 10\%$) for LAI retrieved from date 29/06 to date 09/08 in the inversion of alfalfa and corn surfaces. We found that the effect on alfalfa was negligible, whereas the retrieved LAI of corn field differs by ± 0.3 . For the Barrax region, the effect of soil background variability does not appear to be a major source of error. The particular cases of

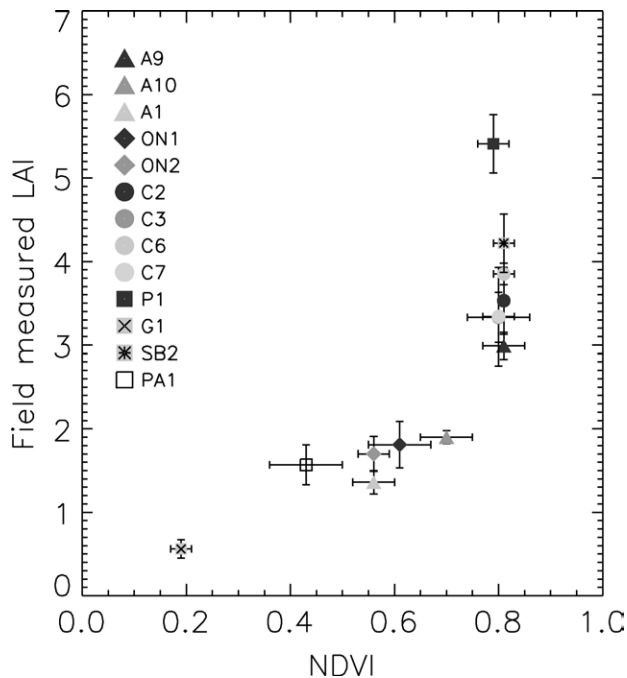


Fig. 12. Relationship between NDVI and in-situ LAI. A stands for Alfalfa; C stands for Corn; G stands for Garlic; ON stands for Onion; P stands for Potato; PA stands for Papaver and SB stands for Sugar Beet.

recent rainfall and recently irrigated fields could not be taken into account in this study, except through the a posteriori examination of the time profiles.

5. Discussion

In this study, we have retrieved LAI from Landsat data, on a pixel basis, for 12 images from March to September 2003 in the agricultural region of Barrax, a semi-arid region with a diversity of crop types and crop growth cycles.

The results are compared with in-situ LAI measurements available in mid July, with very good agreement but a slight bias. The LAI temporal variation of the analysed fields shows consistency with the crop phenological stages for most crop types with the exception of corn and sugar beet fields where some fluctuations in the retrieved LAI are found during a period when LAI is typically high.

Several issues are discussed below in a broader context.

5.1. Effective LAI

Green LAI is defined for flat leaves as the sum of the one-sided green leaf area per unit ground area (Chen & Black, 1992). In plants, leaves are usually grouped together rather than distributed uniformly: this is known as the foliar clumping. The LAI (also called true-LAI) is the “effective” LAI corrected for clumping (Chen, 1996; Lacaze et al., 2002). The LAI “seen” by optical instruments (i.e. Landsat and LAI-2000) is the effective LAI. The scope of this work is to give an estimation of the effective green LAI. Furthermore, optical instruments, which measurements are based on light absorption, are sensitive not only to leaves but also to other plant elements (stems). Thus we

have been abusively using LAI in place of plant area index (Bréda, 2003).

When comparing total LAI destructive measurements with optically-retrieved LAI, discrepancies will be found, in particular for canopy with high LAI. This is due to the clumping effect, and due to the physical saturation of the reflectances in the optical region. The effective LAI is directly linked to the light absorption processes, photosynthesis and evapotranspiration, whereas true LAI is related to carbon allocation and growth processes.

5.2. Empirical relationships (NDVI-LAI) versus model inversion:

To assess the possibility to retrieve LAI using empirical relationships between LAI and vegetation indices, e.g. NDVI, LAI for different fields retrieved at different dates are analysed against NDVI derived from the Landsat images. Fig. 11A shows the retrieved LAI as a function of NDVI for different fields and Fig. 11B shows the curves fitted for a few crop types, together with the LAI-2000 measurements. Fig. 12 shows the NDVI-in-situ LAI relationships (all data). Figs. 11 and 12 confirm that a) the NDVI-LAI relationships are dependent on crop type, because the relationships between reflectances and LAI are affected by the plant structure and leaf properties; b) for a given crop, the sensitivity of NDVI to LAI decreases significantly when LAI exceeds 2 or 3. Secondly, in the NIR band, the vegetation spectra are affected by other vegetation parameters such as leaf dry matter content, leaf angle distribution and other factors (i.e. soil background, angular configuration) causing large uncertainties to the retrieval. Using a model with sufficient spectral bands, we may preserve the sensitivity to LAI of NIR band to access to higher values of LAI compared to NDVI, and separate the effects of different parameters to reduce uncertainties in the retrieval.

The graphs indicate that large uncertainties can be expected when deriving LAI from NDVI using a non-crop-specific relationship, especially at high values of NDVI (0.6 to 0.8).

The main advantage of model inversion in comparison with empirical NDVI-LAI relationship is that LAI can be inverted in a higher range (Figs. 4 and 12). This is important for agriculture as crops can reach high LAI values (Table 2). One possibility to combine the two approaches is to use the crop-specific NDVI-LAI relationships derived from model simulations (such as in Fig. 11.) for a given region. The approach would benefit from the prior crop classification using the time series of satellite data. For our study site, the simulated NDVI-LAI relationships need to be further validated for the whole growth cycle and for their inter-annual variation, before their use in such a semi-empirical retrieval scheme.

5.3. Instrument requirements

To benefit from the whole potential of model inversion techniques, a sufficient number of appropriate spectral bands (i.e. with appropriate central wavelengths and narrow bandwidths) are necessary. The information provided by these bands has to be radiometrically accurate and as much spectrally uncorrelated as possible. The spectral information should be sufficient for aerosol

correction and for decoupling the contribution of chlorophyll and water content. This means that the performance of the model inversion techniques would also depend on the satellite data used. Other current sensors with more and narrower bands (i.e. MODIS or MERIS) have, in return, the problem of spectral signal mixing due to their lower spatial resolution over most agricultural mosaics (heterogeneous landscapes). They may be used to monitor the largest fields but will have a majority of mixed pixels at the regional scale. As the relationship between reflectance and LAI is non-linear, inversions using coarse resolution data under the assumption of spatially homogeneous pixel will introduce a bias on the LAI (Garrigues et al., 2006; Tian et al., 2002). The spatial resolution of Landsat (30 m) is adequate enough to ensure accurate retrievals of LAI in our study area.

For the type of heterogeneous landscape we studied, high spatial resolution is necessary to avoid mixed pixels. Higher temporal frequency is also necessary in the period of fast development of the plants. For instance, in our dataset, a critical period (beginning of May) was missed. The presence of clouds ultimately represents a major limitation for multitemporal studies. A higher frequency of acquisitions for optical data to compensate for potential loss of images due to cloudiness would have a major impact on the applicability of the methodology described in this paper.

In particular, this methodology can be suitable for future missions (GMES Sentinel-2, FORMOSAT-2, VENUS, etc...) which will have better radiometric stability and narrower bands than Landsat but, more importantly, will ensure both the high spatial and temporal resolution necessary for most agricultural landscapes.

Acknowledgments

The ESA technical assistance for SPARC 2003 (Ref. 18307/04/NL/FF) is acknowledged, as well as the help from all the participants of the SPARC campaign for the collection of the ground data during the year 2003. This work has been co-funded by the European Commission shared-cost project DEMETER (contract EVG1-2002-00078). Dr. Rubio's work is supported by the Spanish Ministry of Education and Science (MEC) through a "Ramón y Cajal" contract. We thank Dr. Verhoef and Dr. Jacquemoud for the availability of their models. The authors also wish to thank the Diputación de Albacete ITAP and especially to Amelia Montoro, for providing the phenological data.

References

- Allen, R. G. (2000). Using the FAO-56 dual crop coefficient method over an irrigated region as part of an evapotranspiration intercomparison study. *Journal of Hydrology*, 229(1), 27–41.
- Andrieu, B., Baret, F., Jacquemoud, S., Malthus, T., & Steven, M. (1997). Evaluation of an improved version of SAIL model for simulating bidirectional reflectance of sugar beet canopies. *Remote Sensing of Environment*, 60, 247–257.
- Atzberger, C. (2004). Object-based retrieval of biophysical canopy variables using artificial neural nets and radiative transfer models. *Remote Sensing of Environment*, 93, 53–67.
- Baret, F., & Guyot, G. (1991). Potentials and limits of vegetation indices for LAI and APAR assessment. *Remote Sensing of Environment*, 35, 161–173.
- Berger, M., Rast, M., Wursteisen, P., Attema, E., Moreno, J., Müller, A., et al. (2000). The DAISEX campaigns in support of a future land-surface-processes mission. *ESA Bulletin*, 105, 101–111.
- Bicheron, P., & Leroy, M. (1999). A method of biophysical parameter retrieval at global scale by inversion of a vegetation reflectance model. *Remote Sensing of Environment*, 67, 251–266.
- Boegh, E., Soegaard, H., Broge, N., Hasager, C. B., Jensen, N. O., Schelde, K., et al. (2002). Airborne multispectral data for quantifying leaf area index, nitrogen concentration, and photosynthetic efficiency in agriculture. *Remote Sensing of Environment*, 81, 179–193.
- Bondeau, A., Kicklighter, D. W., & Kadukand, J., and the participants of the Potsdam NPP Model Intercomparison Project. (1999). Comparing global models of terrestrial net primary productivity (NPP): Importance of vegetation structure on seasonal NPP estimates. *Global Change Biology*, 5, 35–45.
- Bréda, N. J. J. (2003). Ground-based measurements of leaf area index: A review of methods, instruments and current controversies. *Journal of Experimental Botany*, 54(392), 2403–2417.
- Brisson, N., Mary, B., Ripoche, D., Jeuffroy, M. H., Ruget, F., Nicoulaud, B., et al. (1998). STICS: A generic model for the simulation of crops and their water and nitrogen balances. I. Theory and parametrization applied to wheat and corn. *Agronomie*, 18, 311–346.
- Chen, J. M. (1996). Optically-based methods for measuring seasonal variation of leaf area index in boreal conifer stands. *Agricultural and Forest Meteorology*, 80, 135–163.
- Chen, J. M., & Black, T. A. (1992). Defining leaf area index for non-flat leaves. *Plant, Cell and Environment*, 15, 421–429.
- Chen, J. M., Pavlic, G., Brown, L., Cihlar, J., Leblanc, S. G., White, H. P., et al. (2002). Derivation and validation of Canada-wide coarse-resolution leaf area index maps using high-resolution satellite imagery and ground measurements. *Remote Sensing of Environment*, 80(1), 165–184.
- Clevers, J. G. P. W., Vonder, O. W., Jongschaap, R. E. E., Desprats, J. F., King, C., Prévot, L., et al. (2002). Using SPOT data for calibrating a wheat growth model under Mediterranean conditions. *Agronomie*, 22, 687–694.
- Combal, B., Baret, F., & Weiss, M. (2002). Improving canopy variables estimation from remote sensing data by exploiting ancillary information. Case study on sugar beet canopies. *Agronomie*, 22, 205–215.
- Combal, B., Baret, F., Weiss, M., Trubuil, A., Macé, D., Pragnère, A., et al. (2002). Retrieval of canopy biophysical variables from bidirectional reflectance. Using prior information to solve the ill-posed inverse problem. *Remote Sensing of Environment*, 84, 1–15.
- Confalonieri, R., & Bechini, L. (2004). A preliminary evaluation of the simulation model CropSyst for alfalfa. *European Journal of Agronomy*, 21, 223–237.
- Dawson, T. P., Curran, P. J., & Plummer, S. E. (1998). LIBERTY-modeling the effects of leaf biochemical concentration on reflectance spectra. *Remote Sensing of Environment*, 65, 50–60.
- Demarez, V., Gastellu-Etchegorry, J. P., Dufrêne, E., LeDantec, V., Mougou, E., Marty, G., et al. (1999). Seasonal variation of leaf chlorophyll content of a temperate forest. Inversion of the PROSPECT model. *International Journal of Remote Sensing*, 20, 879–894.
- Duchemin, B., Hadria, R., Erraki, S., Boulet, G., Maisongrande, P., Chehbouni, A., et al. (2006). Monitoring wheat phenology and irrigation in Central Morocco: On the use of relationships between evapotranspiration, crops coefficients, leaf area index and remotely-sensed vegetation indices. *Agricultural Water Management*, 79, 1–27.
- Duke, C., & Guérif, M. (1998). Crop reflectance estimate errors from the SAIL model due to spatial and temporal variability of canopy and soil characteristics. *Remote Sensing of Environment*, 66, 286–297.
- España, M., Baret, L., Aries, F., Chelle, F., Andrieu, B., & Prévot, L. (1999). Modeling maize canopy 3D architecture application to reflectance simulation. *Ecological Modelling*, 122, 25–43.
- Fang, H., & Liang, S. (2003). Retrieving leaf area index with a neural network method: Simulation and validation. *IEEE Transaction on Geoscience and Remote Sensing*, 41, 2052–2062.
- Fang, H., Liang, S., & Kuusk, A. (2003). Retrieving leaf area index using a genetic algorithm with a canopy radiative transfer model. *Remote Sensing of Environment*, 85, 257–270.

- Fernández, G., Moreno, J., Gandía, S., Martínez, B., Vuolo, F., & Morales, F. (2004). Statistical variability of field measurements of biophysical parameters in SPARC-2003 and SPARC-2004 data campaigns. In H. Lacoste (Ed.), *Proc. of the 2nd CHRIS/Proba Workshop, 28–30 April* Frascati, Italy: ESA/ESRIN ESA SP-578, July 2004.
- Fourty, Th. (1996). Estimation du contenu biochimique d'un couvert végétal à partir de données haute résolution spectrale acquises au niveau satellitaire, Phd, Université Paul Sabatier, Toulouse (France), 169 pages.
- Ganapol, B. D., Johnson, L. F., Hlavka, A., Peterson, D. L., & Bond, B. (1999). LCM2: A coupled leaf/canopy radiative transfer model. *Remote Sensing of Environment*, 70, 153–166.
- Gandía, S., Fernández, G., & Moreno, J. (2004). Retrieval of vegetation biophysical variables from CHRIS/PROBA data in the SPARC campaign. In H. Lacoste (Ed.), *Proc. of the 2nd CHRIS/Proba Workshop, 28–30 April* Frascati, Italy: ESA/ESRIN ESA SP-578, July 2004.
- Gao, W., & Lesht, B. M. (1997). Model inversion of satellite-measured reflectances for obtaining surface biophysical and bidirectional reflectance characteristics of grassland. *Remote Sensing of Environment*, 59, 461–471.
- Garrigues, S., Allard, D., Baret, F., & Weiss, M. (2006). Influence of landscape spatial heterogeneity on the non-linear estimation of leaf area index from moderate spatial resolution remote sensing data. *Remote Sensing of Environment*, 105, 286–298.
- Gitelson, A. A., Viña, A., Ciganda, V., Rundquist, D. C., & Arkebauer, T. J. (2005). Remote estimation of canopy chlorophyll content in crops. *Geophysical Research Letters*, 32, L08403. doi:10.1029/2005GL022688
- Gobron, N., Pinty, B., Verstraete, M. M., & Govaerts, Y. (1997). A semidiscrete model for the scattering of light by vegetation. *Journal of Geophysical Research Atmosphere*, 102(D8), 9431–9446.
- Guanter, L., González-Sanpedro, M. C., & Moreno, J. (2007). A method for the atmospheric correction of ENVISAT/MERIS data over land targets. *International Journal of Remote Sensing*, 28(3&4), 709–728.
- Haboudane, D., Miller, J. R., Pattey, E., Zarco-Tejada, P. J., & Strachan, I. B. (2004). Hyperspectral vegetation indices and novel algorithms for predicting green LAI of crop canopies: Modeling and validation in the context of precision agriculture. *Remote Sensing of Environment*, 90, 337–352.
- Hadria, R., Duchemin, B., Lahrouni, A., Khabba, S., Er-raki, S., Dedieu, G., et al. (2006). Monitoring of irrigated wheat in a semi-arid climate using crop modelling and remote sensing data: Impact of satellite revisit time frequency. *International Journal of Remote Sensing*, 27(5–6), 1093–1117.
- Hosgood, B., Jacquemoud, S., Andreoli, G., Verdebout, J., Pedini, G., & Schumck, G. (1995). *Leaf optical properties experiment 93 (LOPEX93)*. Ispra, Italy: European Commission.
- Jacquemoud, S., & Baret, F. (1990). PROSPECT: A model of leaf optical properties spectra. *Remote Sensing of Environment*, 34, 75–91.
- Jacquemoud, S., Baret, F., Andrieu, B., Danson, F. M., & Jaggard, K. (1995). Extraction of vegetation biophysical parameters by inversion of the PROSPECT+SAIL models on sugar beet canopy reflectance data. Application to TM and AVIRIS sensors. *Remote Sensing of Environment*, 52, 163–172.
- Jacquemoud, S., Ustin, S. L., Verdebout, J., Schmuck, G., Andreoli, G., & Hosgood, B. (1996). Estimating leaf biochemistry using the PROSPECT leaf optical properties model. *Remote Sensing of Environment*, 56(3), 194–202.
- Jochum, A., & Calera, A. (2006). Operational Space-Assisted Irrigation Advisory Services: Overview Of And Lessons Learned From The Project DEMETER. *Proceedings of the International Conference on Earth Observation for vegetation monitoring and water management. Naples, Italy, 10–11 November 2005. AIP Conference Proceedings, August 23, 2006, Volume 852*. (pp. 3–13).
- Kimes, D. S., Knyazikhin, Y., Privette, J. L., Abuelgasim, A. A., & et Gao, F. (2000). Inversion methods for physically-based models. *Remote Sensing Reviews*, 18, 381–439.
- Kneubühler, M. (2002). Spectral assessment of crop phenology based on spring wheat and winter barley. Phd, Remote Sensing Laboratories, Department of Geography, University of Zurich, in Remote sensing series, 38. ISBN 3-03703-004-6.
- Koetz, B., Baret, F., Poilve, H., & Hill, J. (2005). Use of coupled canopy structure dynamic and radiative transfer models to estimate biophysical canopy characteristics. *Remote Sensing of Environment*, 95, 115–124.
- Kuusk, A. (1995). A fast invertible canopy reflectance model. *Remote Sensing of Environment*, 51, 342–350.
- Lacaze, R., Chen, J. M., Roujean, J. -L., & Leblanc, S. G. (2002). Retrieval of vegetation clumping index using hot spot signatures measured by POLDER instrument. *Remote Sensing of Environment*, 79, 84–95.
- Lanjeri, S., Meliá, J., & Segarra, D. (2001). A multi-temporal masking classification method for vineyard monitoring in central Spain. *International Journal of Remote Sensing*, 22, 3167–3186.
- Launay, M., & Guerif, M. (2005). Assimilating remote sensing data into a crop model to improve predictive performance for spatial applications. *Remote Sensing of Environment*, 111, 321–339.
- Lauvemet, C., & Baret, F. (2005). Improved estimates of vegetation biophysical variables from MERIS TOA images by using spatial and temporal constraints. *9th International Symposium on Physical Measurements and Signatures in Remote Sensing, ISPMRS, Beijing, 2005*.
- Le Maire, G., François, C., & Dufrêne, E. (2004). Towards universal broad leaf chlorophyll indices using PROSPECT simulated database and hyperspectral reflectance measurements. *Remote Sensing of Environment*, 89, 1–28.
- Miller, J. R., Berger, M., Jacquemoud, S., Moreno, J., Mohammed, G., Moya, I., et al. (2004). Overview of FluorMOD: A project to develop an integrated leaf-canopy fluorescence simulation model. *2nd International Workshop on Remote Sensing of Vegetation Fluorescence, 17–19 Nov. 2004, Montreal (Canada)*.
- Montaldo, N., & Albertson, J. D. (2003). Multi-scale assimilation of surface soil moisture data for robust root zone moisture predictions. *Advances in Water Resources*, 26, 33–44.
- Moreno, J., & participants of the SPARC campaigns. (2004). The SPECTRA Barrax Campaign (SPARC): Overview and first results from CHRIS data. In H. Lacoste (Ed.), *Proc. of the 2nd CHRIS/Proba Workshop* Frascati, Italy: ESA/ESRIN 28–30 April, ESA SP-578, July 2004.
- Nilson, T., & Kuusk, A. (1989). A reflectance model for the homogeneous plant canopy and its inversion. *Remote Sensing of Environment*, 27, 157–167.
- Norman, J. M., Kustas, W. P., & Humes, K. S. (1995). A two-source approach for estimating soil and vegetation energy fluxes from observations of directional radiometric surface temperature. *Agricultural and Forest Meteorology*, 77, 263–293.
- Qin, W., Gerstl, S. A. W., Deering, D., & Goel, N. S. (2002). Characterizing leaf geometry for grass and crop canopies from hotspot observations: A simulation study. *Remote Sensing of Environment*, 80, 100–113.
- Qi, J., Kerr, Y. H., Moran, M. S., Weltz, M., Huete, A. R., Sorooshian, S., et al. (2000). Leaf area index estimates using remotely sensed data and BRDF models in a semiarid region. *Remote Sensing of Environment*, 73, 18–30.
- Spitters, C. J. T., Van Keulen, H., & Van Kraalingen, D. W. G. (1989). A simple and universal crop growth simulator: SUCROS87. Simulation and system management in crop protection. In R. Rabbinge, S. A. Ward, & H. H. Van Laar (Eds.), *Simulation Monographs* (pp. 147–181). Wageningen: Purdoc.
- Tarantola, A. (2005). *Inverse problem theory and methods for model parameter estimation*. SIAM (Society for Industrial and Applied Mathematics). ISBN:0-89871-572-5 342 pp.
- Tian, Y., Wang, Y., Zhang, Y., Knyazikhina, Y., Bogaert, J., & Myneni, R. B. (2002). Radiative transfer based scaling of LAI/FPAR retrievals from reflectance data of different resolutions. *Remote Sensing of Environment*, 84, 143–159.
- Turner, D. P., Cohen, W. B., Kennedy, R. E., Fassnacht, K. S., & Briggs, J. M. (1999). Relationships between leaf area index and Landsat TM spectral vegetation indices across three temperate zone sites. *Remote Sensing of Environment*, 70, 52–68.
- Verhoef, W. (1984). Light scattering by leaf layers with application to canopy reflectance modelling: The SAIL model. *Remote Sensing of Environment*, 16, 125–141.
- Verhoef, W. (2002). Improved modelling of multiple scattering in leaf canopies: The model SAIL++. *Proceedings of the 1st International Symposium on Recent Advances in Quantitative Remote Sensing, 16–20 September 2002* (pp. 11–20). Spain: Torrent.
- Verhoef, W., & Bach, H. (2003). Simulation of hyperspectral and directional radiance images using coupled biophysical and atmospheric radiative transfer models. *Remote Sensing of Environment*, 87, 23–41.

- Viña, A., Gitelson, A. A., Rundquist, D. C., Keydan, G., Leavitt, B., & Schepers, J. (2004). Monitoring maize (*Zea mays* L.) phenology with remote sensing. *Agronomy Journal*, 96, 1139–1147.
- Weiss, M., & Baret, F. (1999). Evaluation of canopy biophysical variable retrieval performances from the accumulation of large swath satellite data. *Remote Sensing of Environment*, 70, 293–306.
- Weiss, M., Baret, F., Myneni, R. B., Pragnère, A., & Knyazikhin, Y. (2000). Investigation of a model inversion technique to estimate canopy biophysical variables from spectral and directional reflectance data. *Agronomie*, 20, 3–22.
- Zhang, Q., Xiao, X., Braswell, B., Linder, E., Baret, F., & Moore III, B. (2005). Estimating light absorption by chlorophyll, leaf and canopy in a deciduous broadleaf forest using MODIS data and a radiative transfer model. *Remote Sensing of Environment*, 99, 357–371.